Grigore Burdea
Jiachen Zhuang
Edward Roskos
Deborah Silver
and Noshir Langrana
Core Bldg., CAIP Center,
Rutgers—The State University of New Jersey
Post Office Box 1390
Frelinghuysen Road
Piscataway, New Jersey 08855-1390

A Portable Dextrous Master with Force Feedback

Abstract

Dextrous masters control robots and artificial environments through hand gestures. Commercial products have open-loop control, without force feedback to the operator. There is a need for portable systems that have force feedback, but are still sufficiently compact to be desktop. In this paper we discuss a prototype master providing force feedback for the Dataglove. The master structure and its actuator characteristics are presented first. Then a control model is given based on finger parameters and joint coupling. The glove calibration is subsequently discussed, taking into account the influence of the feedback structure. The experimental setup and initial results are presented last.

1 Introduction

The teleoperation of multifinger robot hands (Bekey, Tomovic, & Zalikovic, 1990; Jacobsen, Iversen, Knutti, Johnson, & Biggers, 1986; Salisbury, 1985; Venkataraman & Iberall, 1990) requires a dextrous master that is a multi-DOF controller worn on the operator's hand. Use of the hand gestures (Pao & Speeter, 1989) is a natural form of control that can bring significant improvements in teleoperation efficiency. Commercially available dextrous masters (*Dataglove Model 2 Operating Manual*, 1987; Marcus & Churchill, 1988) control the position of a robot hand, or of a simulated hand (in virtual environment applications), in open-loop without force or touch feedback to the operator.

Studies done using nondextrous masters (Hill, 1976) have shown that the completion time for difficult tasks was reduced by 50% when force sensation was present. This may indicate that force feedback can enhance the performance of dextrous systems as well. Force feedback needs to be distinguished from tactile feedback. Tactile feedback produces a perception of touch/no-touch and some perception of the compliance of the manipulated objects (Patrick, 1990). While useful, touch feedback is not capable of producing total rigidity of motion. Therefore the remote or virtual hand can penetrate the manipulated objects and produce damage. Force feedback uses actuators to control the magnitude of forces on the operator hand and wrist. It too is capable of capturing the effect of object compliance, but it can also produce rigidity of motion (for large feedback forces).

The difficulty in the realization of dextrous masters with force feedback stems from a fundamental conflict between adequate control and human factors as they relate to hand geometry and fatigue (Burdea & Zhuang, 1991). Force feedback provided for each joint of the hand and wrist would require a large number of actuators. Unfortunately, the geometry of the human hand reduces the volume that can accommodate these actuators. A number of prototypes with force feedback have been built (Burdea & Zhuang, 1991; Jacobsen, Iversen, Davis, Potter, & Mclain 1989; Jau, 1989). The feedback actuators used by these masters are either hydraulic (Jacobsen et al., 1989) or electric (Jau, 1989) with placement of the actuators remote from the hand. Thus motion/force is being transmitted through an exoskeleton structure with cables and pulleys. Friction and backdriveability become serious issues and costs are high due to complexity. Therefore their usage is quite limited.

Extending the usage of dextrous masters to areas other than telerobotics, such as virtual environments, medical diagnostics, or video games, will require systems that are compact (desktop), safe, quiet, and less expensive. User safety precludes the use of high-pressure hydraulics, while compactness limits the use of cables, pulleys, and electrical motors. If (a reduced number of) light actuators could be placed locally in the palm where forces are required, then friction and backlash cease being major concerns. The resulting more compact master should also have a reduced cost. Work in this direction was done in Japan (Iwata, 1990) resulting in a desktop master with force feedback. This master has the disadvantage that the user hand is kept on the desk. Therefore large motions such as those allowed by the Dataglove are not possible.

This paper describes a portable dextrous master with force feedback that uses micropneumatic actuators placed in the palm of the Dataglove. The system is light, compact, desktop, and relatively inexpensive. It addresses the needs of certain applications that now operate in open-loop and where the addition of feedback to some degrees of freedom is beneficial. Section 2 describes the master configuration and its actuator characteristics. Section 3 gives a model for the control loop. Section 4 details the glove calibration taking into account the presence of feedback actuators. The experimental setup and initial results are presented in Section 5; concluding remarks are given in Section 6.

2 Master Configuration

Initial studies at Bell Laboratories (Burdea & Speeter, 1989) resulted in a one-degree-of-freedom master used to control the Utah hand. This portable master with force feedback (PDMFF) (Burdea, 1991) had one LVDT position sensor in parallel with a pneumatic actuator. The whole structure was compact enough to be held in the palm with only two fingers, as shown in Figure 1. Forces exerted on objects by the robot hand were determined by observing the difference between flexion and extension tensions in the tendons of the robot thumb. This value was then used to directly drive the value of the piston pressure. After a short learning period, the user was able to grasp objects lightly, or with great force, and feel the grasped object compliance. While these experiments were qualitative in nature, they did show the utility of force information for dextrous teleoperation, even with only one feedback actuator. Considerable deprivation was felt by the users when the loop was opened and no force information was fed back.

2.1 Feedback Structure

After these experiments the concept was extended by building at Rutgers University a feedback structure that integrates several PDMFF type actuators with a Dataglove master. The aim was to provide force feedback for multiple fingers and replace the LVDT sensor with the glove's own position sensors. The resulting compact structure has three actuators placed in the palm. This "direct-drive" system enjoys the same advantages as those used to drive robot arms, namely the absence of cables or pulleys and reduced friction. To allow the abduction–adduction of the fingers (thumb, middle, and index), three sphere joints were placed on a small L-shaped platform attached to the exterior of the glove as shown in Figure 2. Three cylinders were mounted coaxially with these sphere joints, thus allowing for direct connection to air tubes passing through the sphere joints.

Each actuator work envelope $V_{work\ envelope}$ is a portion of a sphere sector due to the sphere joints placed on the palm platform.

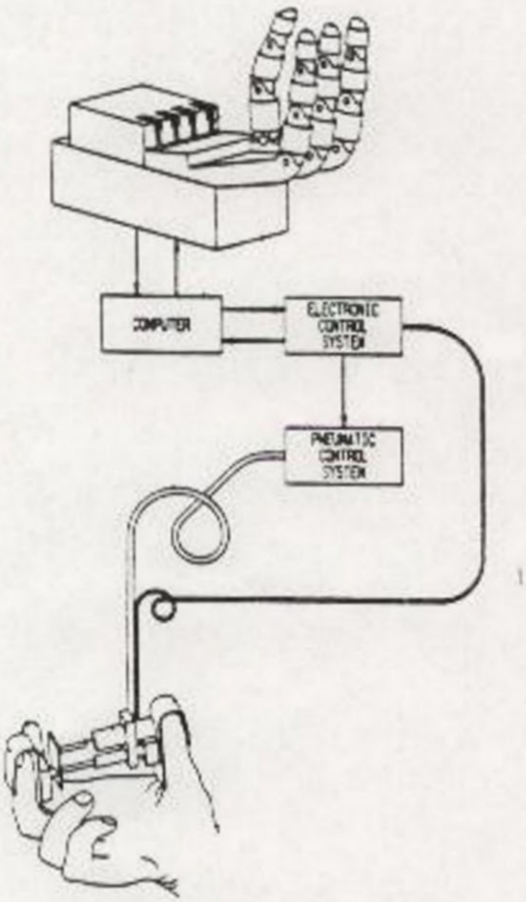

Figure 1. *PDMFF teleoperating the Utah hand (Burdea, 1991).*

$$V_{\text{work-envelope}} = 2\pi d(1 - \cos\alpha)\left[(l + s)^2 + d(l - s) + \frac{d^2}{3}\right] \quad (1)$$

where

d = 20 mm is the piston stroke,
l = 62 mm is the cylinder length,
s = 7 mm is the length of the fingertip mounting block, and
α = 30° is the sphere joint half-angle.

Each cylinder shaft was attached to the glove finger tips through cylindrical joints that allow movement in a plane normal to the fingertips. The attachment of the feedback structure to the glove was done with Velcro® strips mounted in the palm and on the fingers. Each fingertip mounting block had three Velcro strips that secure to the glove. This reduced the compliance of the user fingertip by creating a tight "two-ring" attachment (beneficial to overall system performance). These detachable connections also allowed for adjustments to the hand characteristics of different users.

The actuator controllers and air valves were grouped in a modular hardware interface unit shown in Figure 3. This interface consists of three proportional pressure regulators, a pressure indicator for the main air input, power supply (24 V), and an input port for the cable from a D/A board installed in the host workstation. The interface dimensions are modular with the Dataglove electronic unit so the two units can be "stacked-up" to save desk space.

2.2 Actuator Characteristics

The actuators were tested under both static and dynamic conditions. The static tests were aimed at determining the force exercised by the cylinder as a function of the voltage controlled by the host computer. These tests were run with air supply pressures P_{s}, of 60, 70, 80, and 90 psi and for each supply air pressure voltages from 0 to 10 V were applied on the valve controller. Under these conditions the force was measured with a load cell (accuracy 0.05 N, range 22 N). As seen from Figure 4 the proportionality of force with applied voltage was good, with the exception of plateaus appearing at higher voltages. Here maximum air flow was applied on the piston, and force no longer varied with (increased) voltage. A pressure of 90 psi and a voltage of 6 V resulted in an actuator force of 4 N (almost a pound force). For a fingertip surface of 1.5–2.5 cm^2 this corresponds to 2.66–1.60 N/cm^2. The force generated is therefore 8 to 14 times higher than the minimum sensitivity of the human hand sensors of 0.19 N/cm^2 (Grupen & Henderson, 1986). Plastic was used wherever possible (except for the actuators and sphere joints) to reduce the mass. The cylinder springs were removed to allow free motion of the piston when no air pressure is applied. The resulting feedback structure in the hand had a mass of 0.045 kg (a weight of 0.44 N). Thus for a master total force output of about 13 N, the nondimensional force output/weight ratio is 30. Since the average male/female maximum tip pinching force is 13–16 N (An, Askew, &

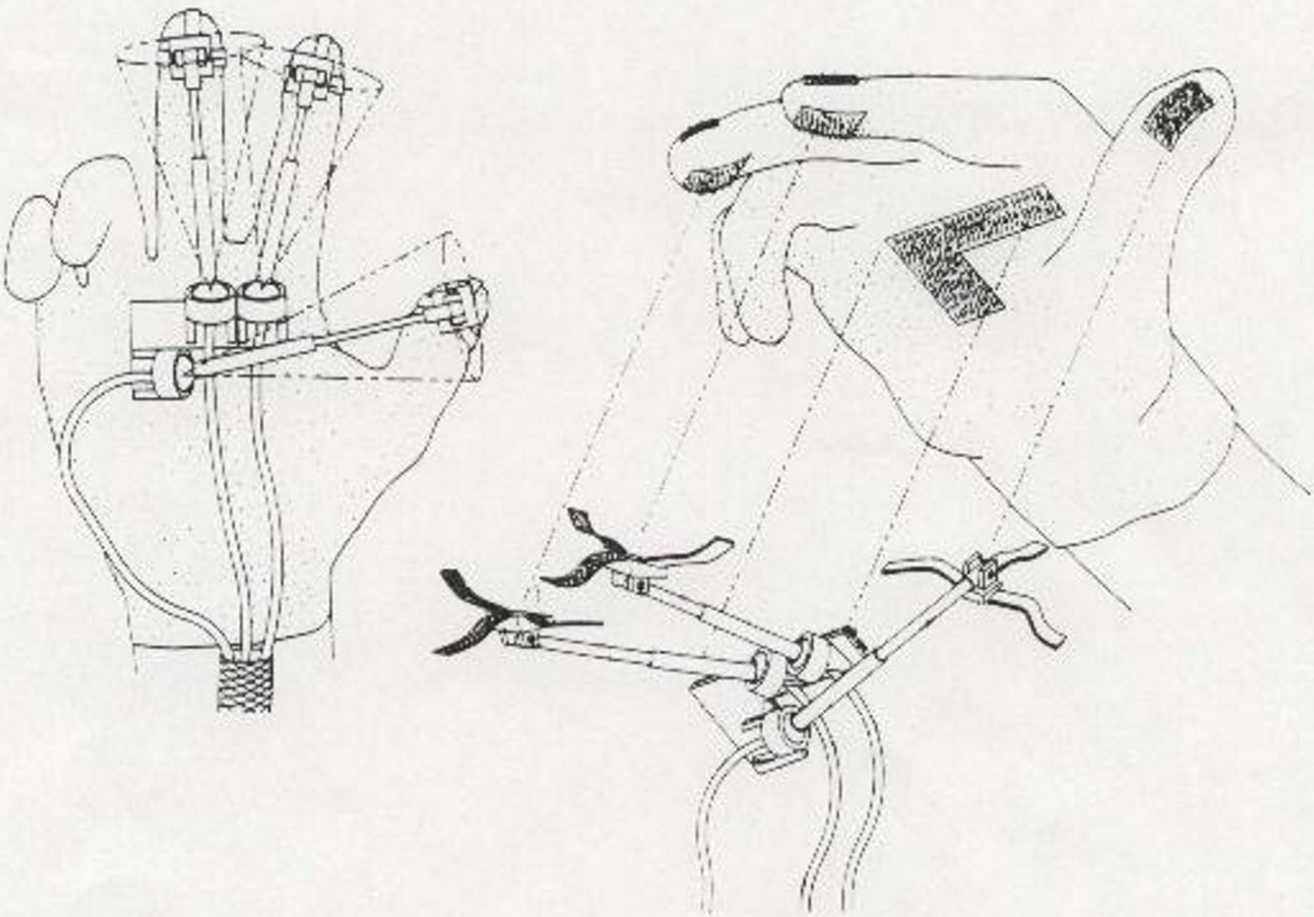

Figure 2. *Force feedback structure for the Dataglove.*

Chao, 1986) the master feedback force is large enough to simulate the sensation of a solid object in the grasp.

The same load cell was subsequently used to determine the force variation in time for a step input. Tests showed an approximately 50–100 msec rise time corresponding to a bandwidth of 10–20 Hz. There were almost no overshoots or oscillations.

The Dataglove uses a magnetic Polhemus [Polhemus Navigation Sciences Division (PNSD), 1987] sensor to measure its palm position and orientation in space. The question arose whether the metallic components in the force feedback structure might interfere with the sensor accuracy. Tests using a calibration table showed this influence on Polhemus accuracy to be quite small (on the order of 1–1.5 mm translation and less than 1° rotation).

3 Control Model

For a given actuator pressure the feedback forces applied on the user fingers depend on two factors, the joint stiffness chosen by the subject, and the user hand posture when actuators are pressurized. The hand posture may be expressed by the angle γ between the normal to the fingertip and the actuator shaft, as shown in Figure 5. For a desired normal feedback force to the thumb, F_N, the corresponding air pressure, P_{air}, is

$$P_{air} = 1.1 \frac{F_N}{A_{air} \cos \gamma} \qquad (2)$$

where

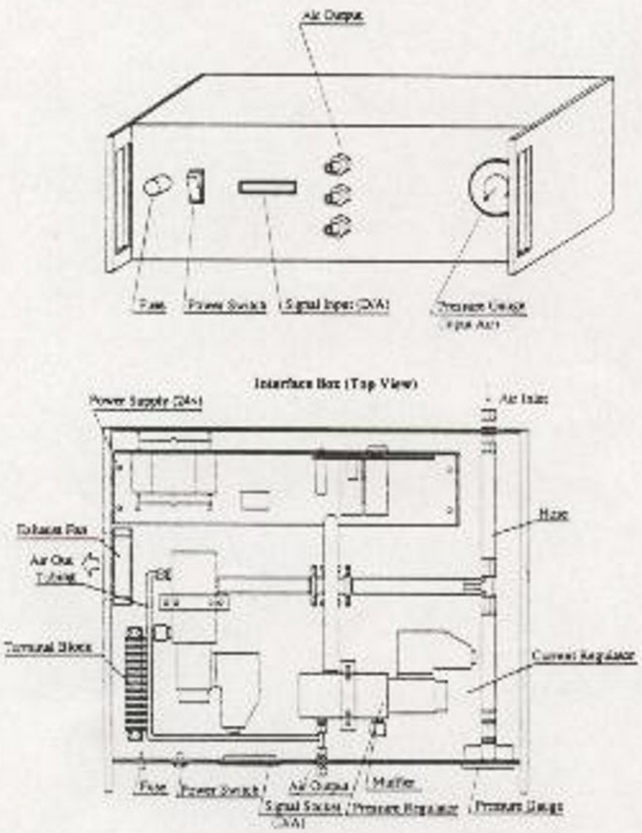

Figure 3. *Feedback interface box.*

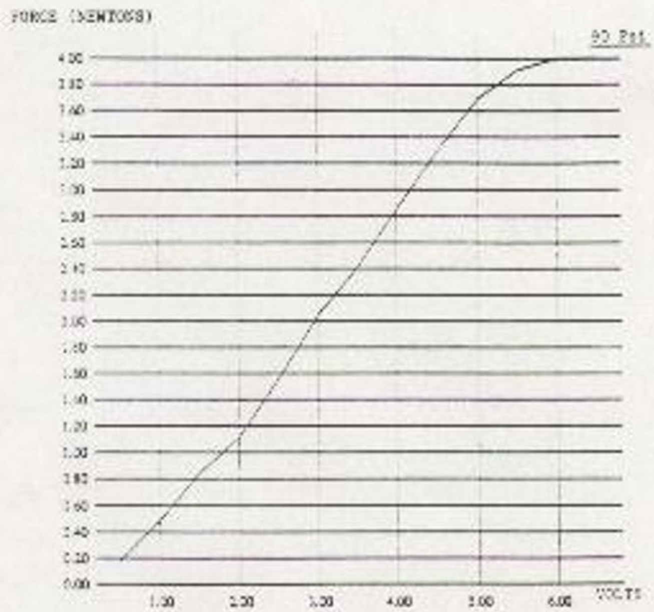

Figure 4. *Microcylinder force measurements (Burdea & Speeter, 1989).*

$$\gamma = 90^\circ - (\theta_1 + \theta_2 + \theta_3) + \tan^{-1}\frac{B_y - H_y}{B_x - L_x} \quad (3)$$

$$B_x = -[L_1 \cos\theta_1 + L_2 \cos(\theta_1 + \theta_2) + L_3 \cos(\theta_1 + \theta_2 + \theta_3) - H_x \sin(\theta_1 + \theta_2 + \theta_3)] \quad (4)$$

$$B_y = L_1 \sin\theta_1 + L_2 \sin(\theta_1 + \theta_2) + L_3 \sin(\theta_1 + \theta_2 + \theta_3) + H_y \cos(\theta_1 + \theta_2 + \theta_3) \quad (5)$$

Here θ_1 is the thumb anteposition/retroposition angle and θ_2, θ_3 are joint flex angles. While the thumb angles are all measured by the Dataglove, the θ_3 angles for middle and index fingers are not measured by the glove directly. One way of determining θ_3 is to take into account the coupling $\theta_3 = \Theta(\theta_2)$ that exists over the range of a grasping motion of the master. θ_3 was found to have the general formula:

$$\theta_3 = \Theta(\theta_2) = a + b\,\theta_2 - c\,\theta_2^2 \quad (6)$$

The constants a, b, and c depend on each user hand characteristics. Data used to obtain Eq. (6) are presented in Figure 6 (pointer $a = 9.32$, $b = 0.22$, and $c = 0.017$; middle finger $a = 9.77$, $b = 0.36$, and $c = 0.014$). For the index and middle fingers Eqs. (3–5) become

$$\gamma = 90^\circ - [\theta_1 + \theta_2 + \Theta(\theta_2)] + \tan^{-1}\frac{B_y - H_y}{B_x - L_x} \quad (7)$$

$$B_x = -[L_1 \cos\theta_1 + L_2 \cos(\theta_1 + \theta_2) + L_3 \cos[\theta_1 + \theta_2 + \Theta(\theta_2)] - H_x \sin[\theta_1 + \theta_2 + \Theta(\theta_2)]] \quad (8)$$

$$B_y = L_1 \sin\theta_1 + L_2 \sin(\theta_1 + \theta_2) + L_3 \sin[\theta_1 + \theta_2 + \Theta(\theta_2)] + H_y \cos[\theta_1 + \theta_2 + \Theta(\theta_2)] \quad (9)$$

In a virtual environment application the normal forces F_N correspond to contact forces resulting from the modeled hand (see Section 5) grasping of an object. Contact forces may depend on the stiffness K of the simulated object, its weight, as well as the hand grasping posture and the degree of squeezing expressed by the motion Δx of the model hand fingertips. The process starts with the

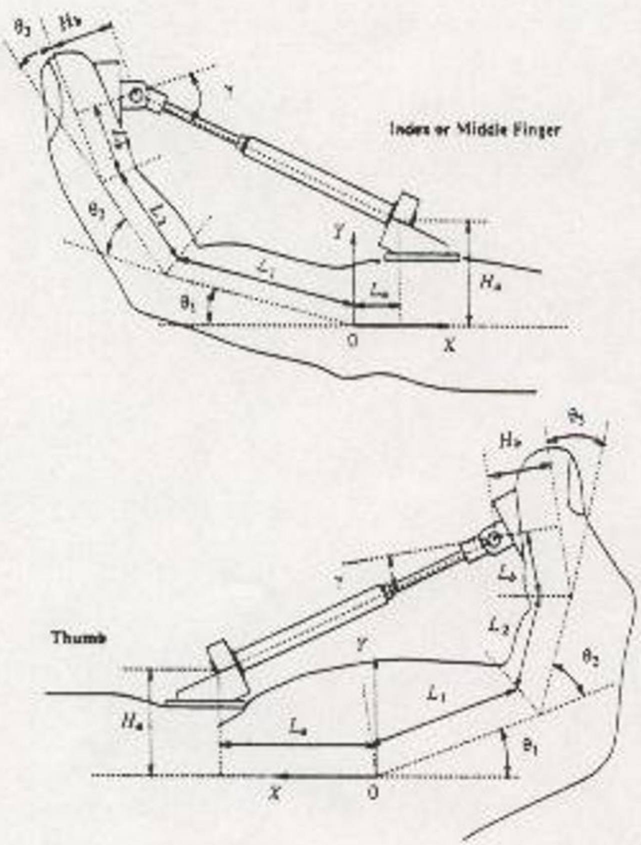

Figure 5. Finger parameters.

master measuring the user finger joint angles θ_i, and the host computer calculating fingertip Cartesian motions ΔX_i. Once the object is grasped, the normal forces, F_{N_i}, are calculated for the three fingers based on the object compliance K. Then air pressures, P_{air}, are calculated for γ_i and F_{N_i}. Forces are then applied on the subject's fingers resulting in a possible new motion command, changing θ_i. This is a position feedforward-force feedback loop, as shown in Figure 7.

4 Glove Calibration

The Dataglove uses optical sensors to measure the finger angles of the operator hand. The glove used in the experiments presented here had added sensors for adduction/abduction and retroposition/anteposition angles. The sensor identification numbers are shown in Figure 8.

The calibration process transforms raw sensor data into user hand joint angles. The main method used in these calibrations was the least squares approximation. However, the method used for flex and anteposition/retroposition angles differs from that used for adduction/abduction sensors. Table 1 summarizes the calibra-

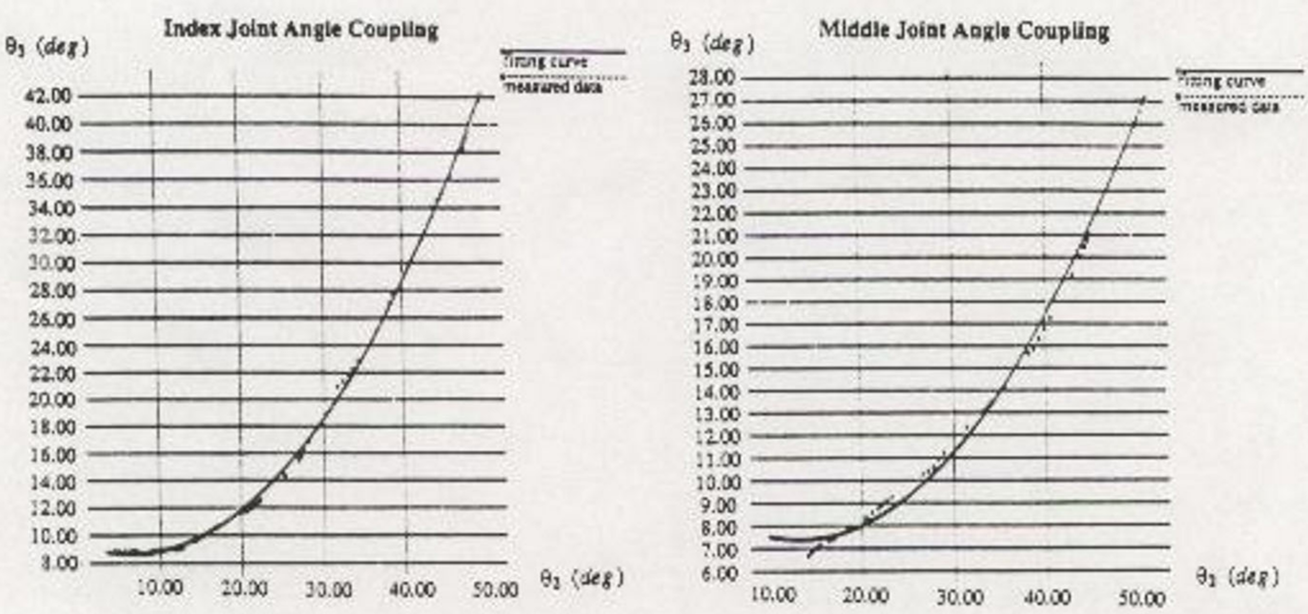

Figure 6. θ_3 and θ_2 coupling for the index and middle fingers.

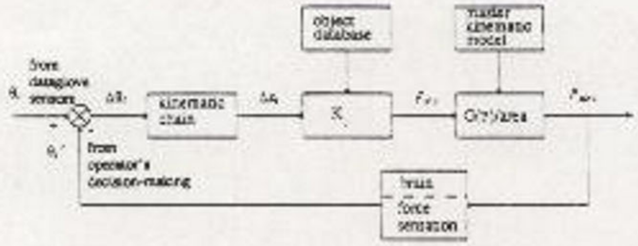

Figure 7. *Control loop.*

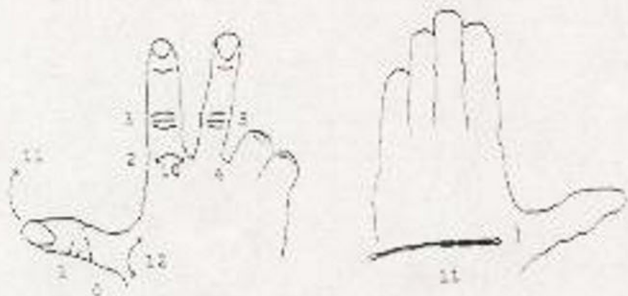

Figure 8. *Numbering of joint sensors used by the Dataglove.*

tion methods for the various joints of the glove discussed presently.

4.1 Flex Sensor Calibration

The flex sensor method of calibration applies to the flexion joints of the thumb, index, and middle fingers and the anteposition/retroposition joint of the thumb. The "zero" position for these angles corresponds to the palm and fingers placed straight on a flat surface. As the fingers bend they form positive angles through the range of motion of the hand. The calibration formula used in our experiments is that given by Hong and Tan (1988)

$$\theta(r) = a + b\,r + c \ln(r) \tag{10}$$

where

r = raw sensor readings

$\theta(r)$ = flex angles

a, b, and c are constants determined via least squares method.

The resulting equation can be expressed as

$$\begin{bmatrix} m & \Sigma r_i & \Sigma \ln(r_i) \\ \Sigma r_i & \Sigma r_i^2 & \Sigma r_i \ln(r_i) \\ \Sigma \ln(r_i) & \Sigma r_i \ln(r_i) & \Sigma[\ln(r_i)]^2 \end{bmatrix} \begin{bmatrix} a \\ b \\ c \end{bmatrix} = \begin{bmatrix} \Sigma r_i \\ \Sigma r_i \theta_i \\ \Sigma \theta_i \ln(r_i) \end{bmatrix} \tag{11}$$

Table 1. *Calibration Methods and Range of Motion (ROM)*

Joint number	Method of calibration	ROM w/o actuator	ROM w/actuator	n_i	d_i
0	Flexion	0–90	15–40	3.6	−54
1	Flexion	0–90	0–90	1	0
2	Flexion	0–90	0–30	3	0
3	Flexion	0–90	0–45	2	0
4	Flexion	0–90	0–30	3	0
5	Flexion	0–90	0–45	2	0
10	Adduct/abduct	0–30	0–30	1	0
11	Flexion	0–90	0–50	1.8	0
12	Adduct/abduct	0–50	0–50	1	0

where

a, b, and c are calibration constants

θ_i are the measured angles

r_i are flex sensor readings

m is the number of data points.

4.2 Adduction/Abduction Sensor Calibration

The calibration for the adduction/abduction sensors is more involved than that of the flex sensors since there is coupling with the flex sensors. Consider a finger with a flexion sensor and an adduction/abduction sensor. θ_f is the flexion sensor angle and θ_a is the adduction/abduction sensor angle. The calibration model assumes that θ_f is not dependent on θ_a and implicitly the raw sensor value r_f is not dependent on r_a. Let us define a function

$$r_{a0} = \phi(r_f) \tag{12}$$

where r_{a0} is used to represent a value of r_a when θ_a is zero degrees. The function ϕ can be found using a least-squares curve fit given a set of values for r_f and r_{a0}. It is possible to collect data while slowly moving the finger against a thin rigid plate at $\theta_a = 0$ and various values of r_f.

Once ϕ has been found, a calibration formula can give θ_a for an arbitrary reading r_a. Let us define this function as

$$\theta_a = \phi(r_{a0} - r_a) \quad (13)$$

The idea behind an argument of $r_{a0} - r_a$ is that of subtracting the effect of the flex sensor from the abduction sensor (it is an approximation that does not lead to significant loss in accuracy). The accuracy after calibration was 4–7° error for flexion angles, 5–8° for adduction/abduction, and 6–8° for anteposition/retroposition.

The feedback actuators placed in the palm reduce somewhat the range of motion of the user's hand (see Table 1). This reduction is significant only for the flexion angles of the index and middle fingers. However, it is possible to scale these angles into a full range of motion of the virtual hand. The scaling function could take on several forms as long as the full range of motion with the actuators in place maps to the full range of motion without the actuators in the palm. For instance, the master angles θ_i could be linearly scaled to the virtual hand angles α_i as represented in Eq. (14).

$$\alpha_i = d_i - n_i \theta_i \quad (14)$$

The constants d_i and n_i are summarized in Table 1. The scaling process also affects the accuracy of the virtual hand position since sensor errors are scaled as well.

5 Experimental Setup and Initial Results

The configuration of the experimental system used to integrate the master in a virtual environment is shown in Figure 9. The actuator interface box was integrated into the system via a D/A board connected to a Sun 4 host. The VPL interface box was also connected to the same Sun 4 while a separate HP 9000 series 300 workstation was used for three-dimensional (3-D) graphics. A second Sun 4 workstation was used as a database server for the other two computers. Intercommunication between computers was done over the ethernet and utilized a master/slave process distribution. Two processes, Vplserv and Dacserv, provided the software interface for the actuator and VPL boxes to other machines on the network. Glove angles were received on the HP workstation by the program Vpleli, which creates a shared memory segment into which the glove data was stored. The graphics program hand attached to this memory segment in order to obtain real-time Dataglove data, then interfaced with Dacserv to relay actuator update forces to the voltage-controlled air valves. User specific calibration data and virtual object models were furnished by Dbserver.

A simple virtual application was constructed to experiment with simulated contact forces. In this application a hand model was displayed on the screen together with modeled objects (see Fig. 10). The objects, depending on their compliance, deformed and returned forces when manipulated. The hand model has been simplified to maintain high refresh rates. The distal and middle phalanges were combined for both the index and middle fingers. Thus, the number of joints was reduced from three to two for both fingers. The finger that had the fewest degrees of freedom was the middle finger. It had two joints with one flexion angle each. The index finger had the same flexion angles as the middle, in addition to an abduction/adduction angle for the metacarpophalangeal joint. The thumb had the degrees of freedom of the index finger and the anteposition/retroposition angle.

The Polhemus sensor data were used to determine the position and orientation of the modeled hand. Six data values provided three palm translations and three rotations. The graphics used the Starbase Graphics Library on the HP-UX System. In Figure 10, the hand appears with a spring attached between the tips of the thumb and middle fingers. As the user's hand and fingers moved, the screen was updated accordingly. The force generated from the compression of the spring was calculated based on Hooke's law and fed back to the master. New data from the Dataglove were obtained at about 25 Hz while the graphics model was capable of 10 Hz refresh rate. The user could both see and feel the results of his/her hand motions in a very natural way.

More experimental data are necessary to perform a statistical analysis of user performance with the feedback master. Comparative tests need to be developed to gauge the benefits of the system presented here. This is the subject of current investigation.

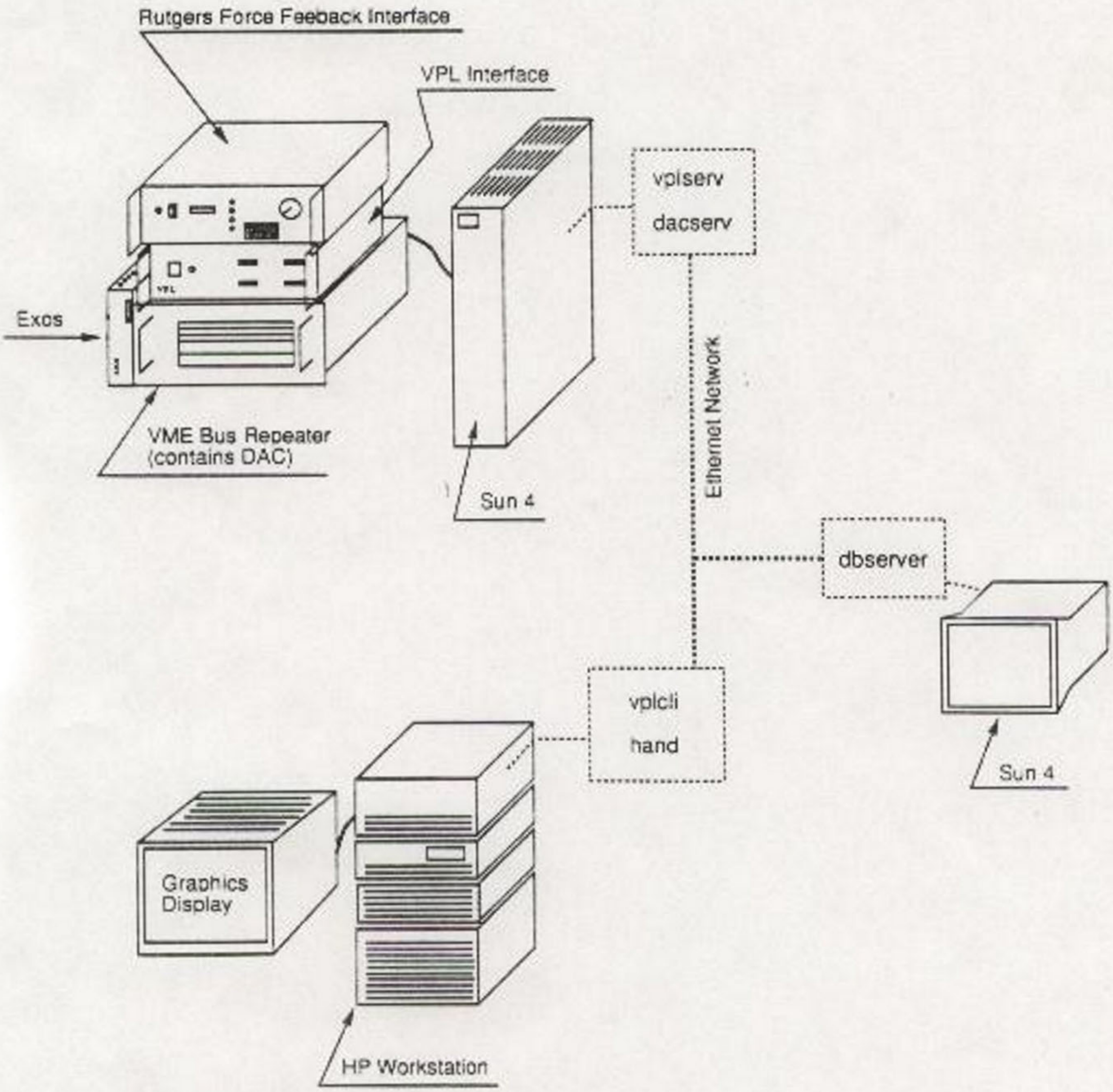

Figure 9. Experimental system set-up.

6 Conclusions

This paper presented a dextrous master with force feedback that uses micro pneumatic actuators placed within the palm of a sensing glove. This system is light, compact, and relatively inexpensive, addressing the needs of certain applications that now operate in open-loop mode but could benefit from a portable feedback device. A kinematic and control model for the master was developed. Calibration methods were obtained taking into account the influence of the feedback structure on the glove range of motion. An initial experiment was presented where the master was integrated with 3-D computer graphics. Although this demo is quite simple, the results are surprisingly realistic and convey the sense of an actual object grasping. Further investigation is

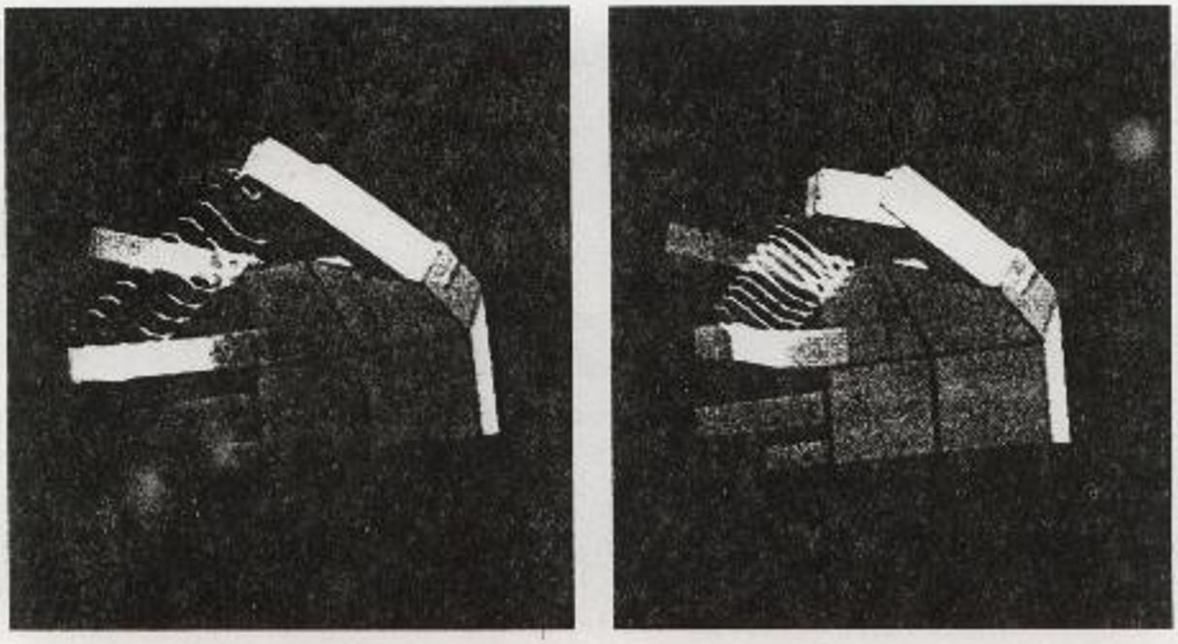

Figure 10. Hand 3-D model with string attached.

needed to develop statistical data for many users and various tasks. Long-term research will address issues related to other fields of application of the device (medical, teleconferencing, and military).

Acknowledgments

The research reported here was supported by the CAIP Center, Rutgers University, with funds provided by the New Jersey Commission on Science and Technology and by CAIP's industrial members, by a Special Purpose Grant from the A.T.&T. Foundation, and by National Science Foundation Grants MSS-89-09335 and CCR-89-09197.

References

An, K., Askew, L.J., & Chao, E.Y. (1986). Biomechanics and functional assessment of upper extremities. *Trends in ergonomics/human factors III* (573–580). Amsterdam: Elsevier Science Publishers B.V.

Bekey, B., Tomovic, R., & Zalikovic, I. (1990). Control architecture for the Belgrade-USC hand. In S.T. Venkataran & T. Iberall (Eds.). *Dextrous Robot Hands* (pages 136–149). New York: Springer-Verlag.

Burdea, G. (1991). Portable dextrous force feedback master for robot telemanipulation. U.S. Patent 5,004,391.

Burdea, G., & Speeter, T. (1989). Portable dextrous force feedback master for robot telemanipulation. *Proceedings 1989 NASA Conference on Space Telerobotics, 2.* Pasadena, CA, 153–161.

Burdea, G., & Zhuang, J. (1991a). Dextrous telerobotics with force feedback—an overview. Part 1: Human factors. *Robotica*. Cambridge, UK., *9*, 171–178.

Burdea, G., & Zhuang, J. (1991b). Dextrous telerobotics with force feedback—an overview. Part 2: Control and implementation. *Robotica*. Cambridge, UK, *9*, 291–298.

Dataglove Model 2 Operating Manual. (1987). Redwood City, CA: VPL Research, Inc.

Grupen, R., & Henderson, T.C. (1986). *A survey of dextrous manipulation.* Tech. Rep., University of Utah.

Hill, J. (1976). *Study to design and develop remote manipulator systems.* (NASA Contract NAS2-8652, SRI Project 4055). Moffett Field, CA: NASA, AMES Research Center.

Hong, J., & Tan, X. (1988). Teleoperating the Utah/MIT hand with a VPL Dataglove I. Dataglove calibration. *Proceedings of 1988 IEEE International Conference on Robotics and Automation.* 1752–1757.

Iwata, H. (1990). Artificial reality with force-feedback: Development of desktop virtual space with compact master manipulator. *Computer Graphics, 24*(4), 165–170.

Jacobsen, S., Iversen, E.K., Knutti, D.F., Johnson, R.T., &

Biggers, K.B. (1986). Design of the Utah/MIT dextrous hand. *Proceedings of 1986 IEEE International Conference on Robotics and Automation*, 1520–1531.

Jacobsen, S., Iversen, E.K., Davis, C.C., Potter, D.M., & Mclain, T.W. (1989). Design of a multiple degree of freedom, force reflective hand master/slave with a high mobility wrist. *Third Topical Meeting on Robotics and Remote Systems.*

Jau, B. (1989). The Jau-JPL anthropomorphic telerobot. *Proceedings NASA Conference on Space Telerobotics, IV*, Pasadena, CA, 75–80.

Marcus, B., & Churchill, P.J. (1988). In A.D. Little (Ed.), *Sensing human hand motions for controlling dextrous robots.*

Pao, L., & Speeter, T. (1989). Transformation of human hand positions for robotic hand control. *Proceedings of 1989 IEEE International Conference on Robotics and Automation*, Scottsdale, AZ, 1758–1763.

Patrick, N. (1990). *Design, construction, and testing of a fingertip display for interaction with virtual and remote environments.* Unpublished master's thesis, MIT, Cambridge, MA.

Polhemus Navigation Sciences Division. (1987). *Space Isotrak user's manual.* Colchester, VT.

Salisbury, J. (1985). Design and control of an articulated hand. In *Design and synthesis* (353–360). Amsterdam: Elsevier Science Publishers B.V.

Venkataraman, S., & Iberall, T. (1990). *Dextrous robot hands.* New York: Springer-Verlag.